OnLine Journal of Biological Sciences

Research Article

Study of the Anatomical, Morphological, and Phytochemical Properties of *Conium maculatum* L.

[1]Aigerim Abdygalieva, [1]Meruyert Sakenovna Kurmanbayeva, [1]Dina Karabalayeva, [2]Zhumagali Ospanbayev, [1,3,4]Moldir Zhumagul, [1]Almagul Aldibekova and [1]Adil Kusmangazinov

[1]Al-Farabi Kazakh National University, Al-Farabi Avenue 71, Almaty, Kazakhstan
[2]Kazakh Scientific Research Institute of Agriculture and Crop Production, Erlepesova Street 1, Almaty, Kazakhstan
[3]Astana Botanical Garden, Orunbur 16, Astana, Kazakhstan
[4]Astana International University, Kabanbai Batyr 8, Astana, Kazakhstan

Article history
Received: 05-12-2024
Revised: 25-12-2024
Accepted: 31-12-2024

Corresponding Author:
Meruyert Sakenovna Kurmanbayeva
Al-Farabi Kazakh National University, Al-Farabi Avenue 71, Almaty, Kazakhstan
Email: kurmanbayevakz@gmail.com

Abstract: The aim of this study is to identify the characteristic anatomical and morphological features and analyze the phytochemical composition of *Conium maculatum* L. growing in the Almaty region, in order to assess the quality of the medicinal plant raw material. Detailed anatomical investigations were conducted, including microscopy of various plant organs (leaves, stems, and roots), as well as phytochemical analysis using chromatographic and spectrophotometric methods. The results revealed that *C. maculatum* from the Almaty region is characterized by a high content of alkaloids, such as coniine and conicine, which possess pronounced toxic properties. The anatomical structure of the plant tissues demonstrates adaptive features related to the influence of local climatic and environmental factors. Furthermore, it was found that the phytochemical composition of the plant varies depending on the growth stages and ecological conditions, which may significantly affect its toxicity levels. The findings of this study are important for the development of safe methods for utilizing *C. maculatum* in pharmaceutical and toxicological practices, as well as for improving the quality of medicinal raw materials.

Keywords: *Conium maculatum* L., Antioxidant, GC-MS Analysis, Coniine, Toxicity, Alkaloids

Introduction

Plants have been used as a source of biologically active substances since antient times. More than a third of all medicinal products are obtained from medicinal plant raw materials. The structure of most biologically active substances is so complex that plants are often their only source. Although thousands of tons of herbal medicinal raw materials are harvested annually in the country, the resulting amount does not satisfy the needs of the pharmaceutical industry (Chizzola and Lohwasser, 2020).

Many plants of the family *Apiaceae* have medicinal properties, due to the high content of coumarins and their derivatives; some species are very poisonous and dangerous for humans and livestock (Sayed-Ahmad *et al.*, 2017).

The genus *Conium* L. (*Apiaceae* Lindl.) is represented by four species commonly found in Europe, Siberia and Asia Minor. One of them is *C. maculatum* growing in Kazakhstan (Ouasti *et al.*, 2024). This is a weedruderal biennial plant with a bare raspberry-spotted stem, up to 2 m high. It blooms in May-June and bears fruit in June-July. It grows as a weed near roads, in orchards, vegetable gardens, in wet ravines of foothills, meadows and occasionally on forest edges in all areas of Kazakhstan, except for deserts (Salem *et al.*, 2021).

C. maculatum is a promising medicinal plant, the aerial part of which is used to treat malignant tumors, diseases of the digestive, respiratory, reproductive, immune, cardiovascular systems, skin diseases, metabolic disorders and pain syndrome (Al-Barwani and Eltayeb, 2004).

The toxic properties of *C. maculatum* have been known since the time of Hippocrates and the plant is still widely used in folk medicine in many countries. *C. maculatum* contains various groups of biologically active substances (flavonoids, furanocoumarins, polyacetylenes, saponins, essential oils, etc. (Vetter, 2004) which explains a wide range of its medicinal properties (Madaan and Kumar, 2012).

Conium L. is known for its toxic properties, which are associated with the presence of many pyridine alkaloids of the first group, which have been isolated from all plants of the genus *Conium* L. The plant also contains flavonoids, polyacetylenes, saponins, coumarins, etc. *Conium* L. has a wide range of pharmacological activity, due to which folk medicine uses it in most herbal mixes for the treatment of almost all diseases, including oncological ones (Radulovic and Dordevic, 2011). The experience of using this plant in folk medicine indicates its wide therapeutic possibilities: Tincture and juice from the aerial parts are used as an analgesic, sedative, antiasthmatic, anticonvulsant, anticancer and antiinflammatory agent (Begum and Mastan, 2015).

The study of *Conium* L. suspension will make it possible to justify its use as a source of biologically active substances and the possibility of further production (Filonova *et al.*, 2018).

According to the literature, all parts of the plant are poisonous and contain pyridine alkaloids, coumarins (up to 0.6% in stems), flavonoids, monoterpenoids, carbohydrates, etc. Essential oil from leaves (0.1%) and fatty oil from fruits (up to 17.5%) have been isolated. From the beginning of the flowering period to the beginning of fruiting, the plants are most poisonous (Karakasi *et al.*, 2019).

The poisonous properties of *C. maculatum* should be taken into account when harvesting and identifying the raw material. All parts of *C. maculatum* are poisonous due to the alkaloids contained in the plant. The alkaloid coniine is comparable in strength to the curare poison (Jha *et al.*, 2024).

C. maculatum contains the most dangerous alkaloids, the main of which is coniine causing respiratory paralysis. Symptoms of poisoning include dizziness, nausea, speech and swallowing disorders, salivation and skin blanching, later convulsions, ascending paralysis with loss of skin sensitivity, depression of the central nervous system, increasing suffocation leads to respiratory arrest (Mondal *et al.*, 2014).

Most poisonous species are used in both folk and official medicine, because of which there is a threat of poisoning due to their uncontrolled use (Al-Snafi, 2016). The lack of public awareness of poisonous plants, their attractive appearance and fragrant smell, which cause the greatest curiosity in young children in nature, are the main causes of plant poisoning (Dayan, 2024).

In Kazakhstan, *C. maculatum* preparations are not used in practical medicine, but are used in traditional medicine and as a classical homeopathic remedy, although many oncologists recommend introducing *C. maculatum* into anticancer drugs (Grudzinskaya *et al.*, 2020; Venkateswaran *et al.*, 2023; Panter *et al.*, 2017).

Greek and Arab doctors used it to treat immature tumors, relieve swelling and joint pain and treat skin diseases (Alishah *et al.*, 2016).

C. maculatum (*Apiaceae*) has traditionally been used to treat spasmodic disorders, as well as to relieve nervous excitement, rheumatic pain, stomach pain, stomach ulcer pain, nervousness and anxiety (Miloud & Senussi, 2023).

The whole plant is poisonous; the poisonous parts include flowers, leaves, mature fruits, roots, seeds, stems and young shoots, but especially poisonous are roots and seeds (Pimenov, 2017; Durnova *et al.*, 2019; Filonova & Medvedeva, 2017; Hotti *et al.*, 2015; Meier *et al.*, 2015).

Publications that describe individual clinical observations are few, including those describing various symptoms depending primarily on the severity of poisoning. The plant has pronounced antiinflammatory and analgesic properties. The analgesic effects of plant extracts are achieved through the blocking of nicotinic receptors. *C. maculatum* polysaccharides have antiinflammatory, immune-stimulating, wound-healing, emollient, choleretic, enveloping and antitumor properties (Ligacheva *et al.*, 2020).

Currently, key challenges in pharmacy include the search for promising plant sources of biologically active substances, the rational use of natural food raw materials, including non-traditional ones and the need to revive domestic production of medicinal plant raw materials and herbal preparations based on Kazakhstan's resources. In Kazakhstan, 1,500 species of medicinal plants are found, of which more than 500 are used as raw materials. Approximately a thousand species of wild medicinal plants in Kazakhstan's flora remain underexplored and present significant scientific interest. Their chemical composition is largely unknown and they have been poorly studied pharmacognostically, which hinders the expansion of the arsenal of plant-derived medicines with modern pharmaceutical preparations.

In this regard, it is crucial to study species with medicinal properties. One such plant is the biennial *Conium maculatum* L. (*Apiaceae* Lindl.), which grows in Kazakhstan.

The purpose of this study was to identify the characteristic morphological and anatomical features and analyze the phytochemical composition, allowing to diagnose medicinal plant raw material of *C. maculatum* in the conditions of the Almaty region.

Materials and Methods

Plant Materials

Populations of *C. maculatum* from four different districts of the Almaty region were sampled. Population B1 was located at the foot of the Karasai Ridge, Zailiysky Alatau, near the 'Yrys' farm in the Rayymbek rural district, N 4319’48.70″, E 7670’54.91″

approximately 2-3 kilometers from the village of Rayymbek and was collected on May 13, 2020. Population B2 was 1 km northwest of the village of Enbekshi, at the foot of the Kuldzhinsky tract, Zailiysky Alatau, N 4315’26.52″, E7690’47.04″ and was collected on July 1, 2021. Population B3 was about 2.4 km southeast of the village of Zhandosovo, Zailiysky Alatau, 4317’10.68″, 7656’84.20″ and was sampled on July 14, 2020. Population B4 was located in the Talgar Range area, Trans-Ili Alatau, Logunov Gorge, approximately 6.7 km north of the village of Talgar and was collected from the Almaty Reserve on July 10, 2021 (Fig. 1).

Fig. 1: C. Maculatum in nature

The Paraffin Methods

Dehydration: The chemicals used for sample dehydration and their exposure times are listed (Table 1).

Table 1: Chemicals used for dehydrating and their exposure times

Chemical substance	Time, min
Ethyl alcohol 80%	20
Ethyl alcohol 96%	10
2 Ethyl alcohol + 1 xylene	20
1 Ethyl alcohol + 1 xylene	20
1 Ethyl alcohol + 2 xylene	20
Pure xylene	5

Infiltration: The paraffinxylene mixture at a ratio of 1:2 was added to the samples after dehydration. It was then stored in closed bottles at 65°C. After waiting for a day, the bottle caps were opened, paraffin was added and the saturation process continued until the xylene odor disappeared.

Embedding: After complete saturation with paraffin, suitable for dissecting (pretreated with glycerol) samples were placed in iron containers, which were then filled with molten paraffin to produce paraffin blocks. After freezing the paraffin blocks, the samples were separated and stored at 4°C.

Segregation: Paraffin blocks were dissected using a 10-12-micron model of the Shandonfinesse 325 Thermo microtome. The sections were placed in a water bath at a temperature of 50-55°C to allow the folds to flatten. A mixture of glycerol and egg white was then applied to the slides so that the samples adhered to them. After the samples were placed onto slides showing the crosssectional thickness and from which part of the plant they were taken, the samples were allowed to dry.

Staining: Preparation of stains, Safranin: 1 mL of liquid safranin dye was mixed with 100 mL of ethyl alcohol (50%). Fast Green: 100 mL solution is obtained by dissolving 0.2 g of Fast Green dye in 95% ethyl alcohol. Dried samples were exposed to staining substances according (Table 2); the dyes used were safranin and fast green.

Table 2: Chemicals used in staining and the duration of their application

Chemical substance	Exposure time (stem, leaf, bark), min	Exposure time (root, fruite), min
Pure xylene	3	3
3 xylene / 1 ethyl alcohol	5	2.5
2 xylene / 2 ethyl alcohol	5	2.5
1 xylene / 3 ethyl alcohol	5	2.5
ethyl alcohol 96% B	5	2.5
ethyl alcohol 90%	5	2.5
Safranin solution	5	5
ethyl alcohol 90%	5	2.5
Fast Green	0.5	0.5
ethyl alcohol 90%	5	2.5

Preparation of the Cross Sections and Viewing them Under the Microscope

Once the samples had undergone these procedures, they were sealed with Entellan to make them permanent samples. They were examined under a LEICA DM3000 microscope and photographed with a LEICA DFC295 camera.

Since the anatomical studies of this kind have not been previously conducted, in the interpretation of cross-sections we used publications and dissertations on the anatomy of the family Apiaceae (Tamamschian *et al.*, 1969; Bani *et al.*, 2011; Metcalfe and Chalk, 1950; 1957; Akpulat and Ataşlar, 2014; Bani *et al.*, 2016a-b; Mavi İdman *et al.*, 2019; Ulusoy, 2017; Başer and Pehlivan, 2015; Karakaya *et al.*, 2021; Ulusoy *et al.*, 2017; Kurmanbayeva *et al.*, 2024).

Several photographs were taken with a light microscope; to obtain full-size images, the photographs taken were combined in Adobe Photoshop 2020. The cross-sections of the samples from different locations were mapped using CorelDRAW Technical Suite 2022.

Plant Extract Preparation

The dried plants were ground into a fine powder with a mortar and pestle. The preparation of the extracts was carried out at a temperature of 50°C for 30 min using the ultrasonic extraction method. This method was used as a simple and effective way to obtain the extract. The sample volume was 5 mL. The samples were centrifuged for 5 min at 5000 rpm. After filtration with filter paper No. 1, the extracts were evaporated at 60°C using a rotary evaporator. The dried extract samples were resuspended in 2 mL of dichloromethane. Samples were filtered using 0.45 µm hole diameter syringe filters prior to injection into GC-MS.

GC-MS Analysis

Analysis by gas chromatography and mass spectrometry was performed in the GC-MS QP2010 Ultra system (Shimadzu, Tokyo, Japan). A Restek rxi-5 ms column with a length of 30 m; diameter of 0.25 mm; and film thickness of 0.25 µL was used. The column temperature was maintained at 40°C for 1 min after injection and then programmed from 5°C/min to 300°C held for 5 min. The temperature was maintained at 250°C for the ion source and 270°C for the interface. The electron ionization by the mass detector was 70 eV.

Chemical Components Identification

The relative amount of chemical compounds present in each of the extracts was expressed as a percentage based on the peak area size in the chromatogram. Compound detection was performed by searching the mass spectra library (NIST 14) and comparing to the mass spectra data in the literature.

Determination of the Total Amount of Phenolic Compounds

Dried plant samples (0.1 g) were homogenized by a mortar and pestle in 2.5 mL of methanol. The homogenized samples were then incubated at 80°C for 15 min. After incubation, samples were centrifuged at 500 rpm for 10 min. Supernatants were used as extracts to determine the total amount of phenolic compounds after evaporation of the solvent and resuspension of extracts in 1 mL of methanol. To 100 µL of extract of each sample 1 mL of Folin-Ciocalteu reagent was added. The mixture was shaken and incubated at ambient temperature for 15 min, then 1 mL (7.5%) of Na2CO3 solution was added to the mixture and the resulting mixture was incubated at room temperature for 90 min. The absorbance of the samples was measured at a wavelength of 765 nm using a spectrophotometer. The total amount of phenolic compounds is given in µg GAE/mL.

Determination of the Antioxidant Activity

The antioxidant activity of plant extracts was evaluated by the DPPH purification method (2,2 diphenyl-1-picrylhydrazyl). The same extracts (considered 100% extract for the experiment) that were prepared to determine the total amount of phenolic compounds were used to determine the antioxidant activity of the plant samples. Sequential dilution of plant extracts with methanol to 20, 40, 60, 80 and 100% was carried out. Then, 100 µL of extract of each concentration was added to 2.9 mL of 0.1 mm DPPH solution to obtain a final volume of 3 mL. The mixture was then incubated at room temperature for 15 min and the absorption was measured with a 517 nm spectrophotometer. The absorbance activity of DPPH extracts was evaluated by the formula below, where % SA is the per cent of antioxidant activity, ADPPH is the absorbance of DPPH and ASample is the testing sample absorbance:

$$\%SA = \frac{A_{DPPH} - A_{Sample}}{A_{DPPH}} \times 100$$

Results and Discussion

Measuring the Photographs

A total of 42 marks were made, with 12 in one section of the rod and 30 in another. The measured elements are listed in Tables (3-5) and shown in Figure (2).

Root Anatomy

The root has a rounded shape with a diameter of the cross-section of 2.23±0.047 mm and is covered with the periderm. The periderm consists of three layers: Phellem, phellogen and phelloderm. The phellem consists of 3-4 rows of cells. The cortex consists of parenchyma cells of

varying sizes, with an average thickness of 80.72±28.04 µm. The shape and size of the cortical cells vary, reflecting their diversity. There is a secretory duct between these cells. The conductive elements are separated by the cambial tissue. The central cylinder is surrounded by the phloem. Inside the central cylinder is the xylem. The xylem bundles form a radial array and are separated from each other by parenchymal cells (Figure 2).

The phellem consist of 3-4 rows of cells. The cells of phellem are rectangular in shape and 12.6×22.2 µm in size. The phellem is followed by a single layer of phellogen. The phelloderm consists of 2-3 rows of cells (Figure 3). The inner parts of the root contain less phloem and more xylem; there are 1-2 layers of cambium cells between the phloem and xylem and a large amount of xylem inside (Figure 3). The xylem layer consists of oval-shaped tracheids 48.53×66.65 µm in size; the xylem is separated by bundles of parenchymal cells.

Table 3: Measurable root elements

Description	Abbreviations
Root diameter	K1
Root cell width	K2
Root cell length	K3
Phellem cell count	K4
Phellogen cell count	K5
Phelloderm cell count	K6
Root cortex thickness	K7
Number of cortex cells	K8
Root cortex cell width	K9
Root cortex cell length	K10
Root duct width	K11
Root tracheal cell length	K12

Table 4: Root anatomical elements and results of statistical analysis (A, B, C, D: groups; *: significant differences

Description		Almaty Nature Reserve 10.07.2021 (B4) N = 10	Karasai District (Shamalgan) 14.07.2021 (B3) N = 10	Karasai District 13.05.20 (B1) N = 10	Zailiyskiy Alatau 1.07.2021 *(B2)* N = 10
K1	Ort ± Std	2231,1±49,28	2930,9±75,41	2874,2±158,09	2990,4±192,79
	min-max	21442286	2803-3094	2598-3098	2670-3289
	95% CI	2195,852266,3	2876,9-2984,8	2761,1-2987,3	2852,48-3128,32
K2*	Ort ± Std	12,60±1,76^{A}	15,01±2,92^{AB}	16,98±1,6^{B}	22,35 ±3,23^{C}
	min-max	11,016,0	11,019,0	13,019,0	15,026,0
	95% CI	11,313,86	12,9317,10	15,8418,12	20,0424,66
K3*	Ort ± Std	22,15±3,01^{A}	23,89±5,07^{AB}	34,69±4,83^{C}	28,52±5,52^{B}
	min-max	18,026,0	16,033,0	23,040,0	20,039,0
	95% CI	19,9924,31	20,2627,52	31,2438,15	24,5732,47
K4	Ort ± Std	3,5±0,5	3,6±0,51	3,5±0,52	3,50±0,52
	min-max	3,004,00	3,004,00	3,004,00	3,004,00
	95% CI	3,123,88	3,233,97	3,123,88	3,123,88
K5	Ort ± Std	1,00 ±0,00	1,00±0,00	1,00±0,00	1,00±0,00
	min-max	1,00-1,00	1,00-1,00	1,00-1,00	1,00-1,00
	95% CI	1,00 -1,00	1,00-1,00	1,00-1,00	1,00 -1,00
K6*	Ort ± Std	2,50±0,53^{A}	5,10±0,99^{C}	3,00±1,05^{A}	4,00±0,0^{B}
	min-max	2,003,00	4,006,00	2,004,00	4,004,00
	95% CI	2,122,88	4,395,81	2,253,75	4,04,0
K7*	Ort ± Std	80,72±29,55^{A}	325,05 ±35,9-49^{C}	198,41±49,92^{B}	278,98±40,37^{C}
	min-max	35,0130,0	268,0379,0	136,0272,0	221,0356,0
	95% CI	59,58101,86	299,66350,44	162,70234,12	250,10307,86
K8*	Ort ± Std	15,50±0,52^{A}	14,20±1,39^{A}	21,00±1,41^{C}	19,40±1,07^{B}
	min-max	15,0016,00	11,0016,00	19,0024,00	18,0021,00
	95% CI	15,1215,88	13,2015,20	19,9922,01	18,6320,17
K9*	Ort ± Std	6,8±0,78^{A}	13,69±2,35^{B}	13,36±3,29^{B}	21,72±2,05^{C}
	min-max	6,08,0	10,017,00	9,019,0	17,024,0
	95% CI	6,247,36	12,0115,38	11,015,71	20,2523,19
K10*	Ort ± Std	13,24±5,03^{A}	37,32±7,08^{BC}	28,10±5,7^{B}	46,69±12,54^{C}
	min-max	6,020,0	28,051,0	22,041,0	31,070,0
	95% CI	9,6416,84	32,2542,39	24,0232,18	37,7255,66
K11*	Ort ± Std	48,53±7,58^{A}	77,14±15,32^{BC}	75,28±18,90^{B}	92,63±7,14^{C}
	min-max	40,068,0	51,0103,0	30,091,0	86,0109,0
	95% CI	43,1153,96	66,1888,11	61,7588,8	87,5197,74
K12*	Ort ± Std	66,65±13,17^{A}	98,85±20,16^{B}	115,83±16,18^{B}	111,58±27,13^{B}
	min-max	51,093,0	51,0125,0	90,0133,0	84,0151,0
	95% CI	57,2276,07	84,43113,28	104,25127,41	92,18130,99

Table 5: Measured stem elements

Description	Abbreviations
Stem diameter	G1
Thickness of the primary stem cortex	G2
Primary stem cortex thickness (number of cells)	G3
Stem epidermal cell width	G4
Stem epidermal cell size	G5
Stem cortex cell width	G6
Stem cortex cell length	G7
Stem cortex thickness	G8
Stem sheath thickness (number of cells)	G9
Stem sclerenchyma cell width	G10
Stem sclerenchyma cell size	G11
Sclerenchyma thickness (number of cells)	G12
Width of the stem's individual cell	G13
Length of the inner stem cell	G14
Tracheal elements of the stem xylem width	G15
Tracheal elements of the stem xylem length	G16
Stem tracheid cells width	G17
Stem tracheal cell size	G18
Stem serrated ligament width	G19
Stem conductive beam length	G20
Width of the secretory duct	G21
Length of the secretory duct	G22
Total number of conductive beams in the stem	G23
Thickness of the main stem collenchyma (cell number)	G24
Width of the main stem collenchyma	G25
Length of the main root Thickness of the collenchyma	G26
Width of the secretory duct	G27
Length of the secretory duct	G28
Number of cells along the edges of the secretory duct	G29
Total number of the stem secretory ducts	G30

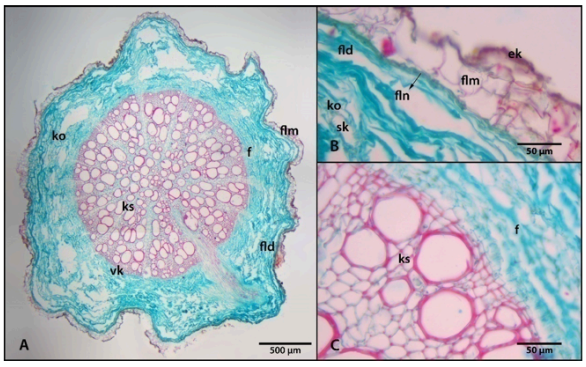

Fig. 2: Root cross-section a) General view B) Periderm C) Main part

Results of the Statistical Analysis

Mean±standard deviation, minimum and maximum values and 95% confidence interval were estimated using ANOVA and Turkey test. The analyses revealed elements that differed significantly between taxa. ANOVA revealed significant differences in nine root elements (Table 4). The Turkey test yielded similar results (Figure 2-4). The following elements were not significantly different: “root diameter” (K1), “phellem cell count” (K4) and “phellogen cell count” (K5).

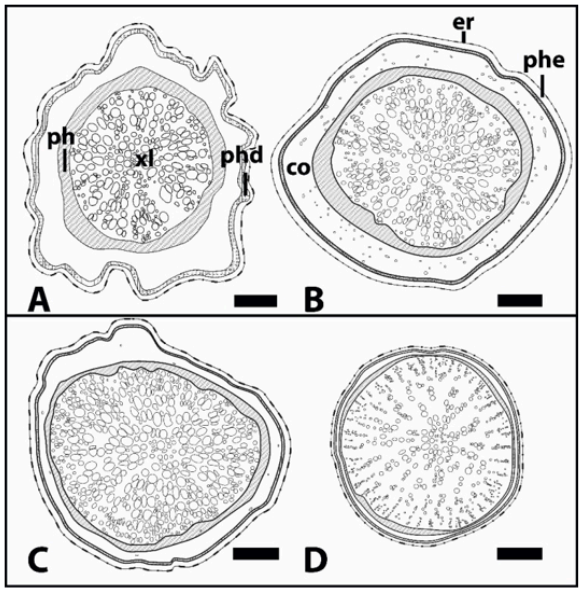

Fig. 3: C. maculatum root diagrams from different areas: A) Trans-Ili Alatau; B) Karasai district (Shamalgan); C) Karasai district; D) Almaty reserve. Scale = 500 µm

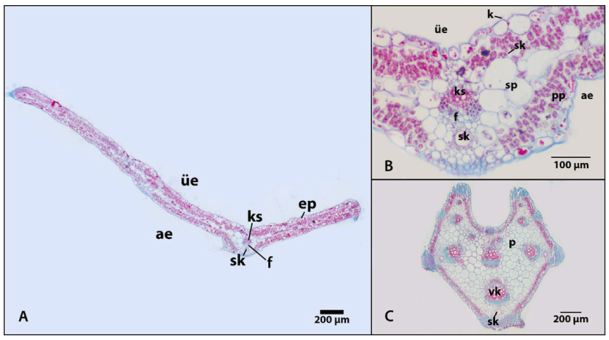

Fig. 4: Leaf cross section: a) General view B) Enlarged image C) Overview

Leaf Anatomy

In the cross-section, the petiole consists of a single row of cells and is surrounded by epidermal cells of different sizes. Under the epidermis, there are three to four rows of sclerenchyma cells (Figure 4). At the corners, there are 12-15 rows of collenchyma cells. Below this layer are vascular bundles that penetrate parenchyma cells and are usually located close to the corners (Figure 5). The conductive beams along the leaf taper off from the center to the sides. At the bottom of the conductive beams facing the epidermis, there are oil granules on the sides of the conductive beams in the middle vessels.

In the cross-section of the leaf, the cuticle and a row of epidermal cells surround the outermost cuticle (Figure 6). The mesophyll consists of 1-2 rows of palisade and spongy parenchyma. In the middle part of the leaf there are oil granules on the abaxial side and a conducting beam above them.

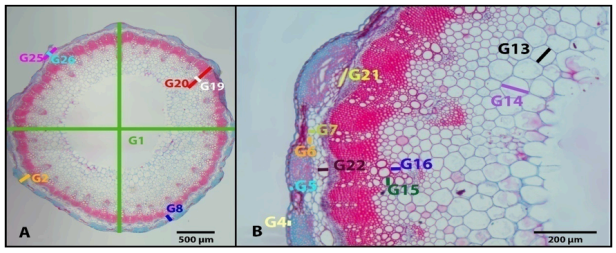

Fig. 5: Characteristics of the plant stem (G1- 30)

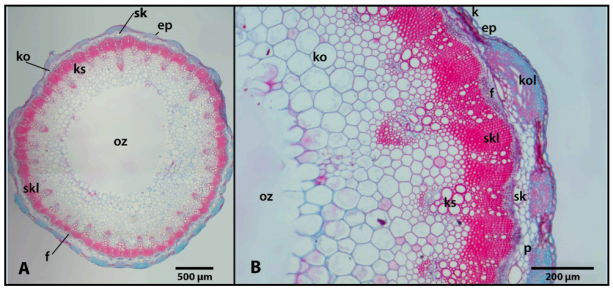

Fig. 6: Stem cross-section A) general view b) close-up

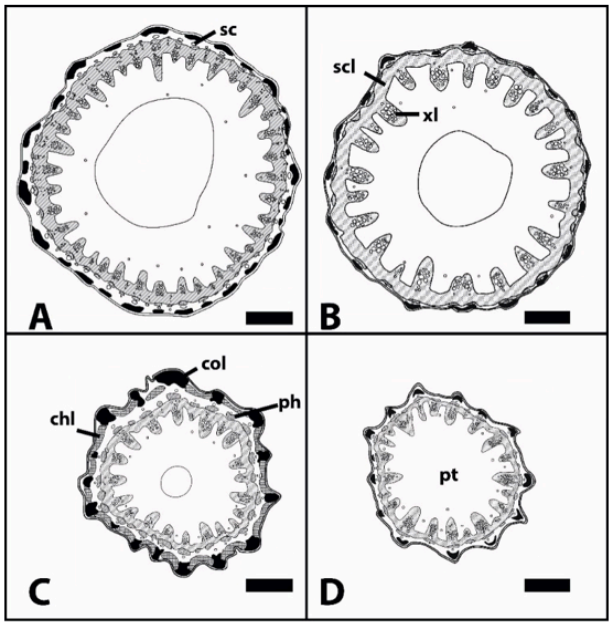

Fig. 7: Conim maculatum L. stem sections from different regions: A) Trans-Ili Alatau; B) Karasai district (Shamalgan); C) Karasai district; D) Almaty reserve. Scale = 500 µm

Stem Anatomy

In the cross-section, the stem was round-elliptical with a diameter of 2.54±0.498 mm. The epidermis is 16.56 ×13.79 µm wide, it consists of a single row of cells with an outer cuticle. Under the epidermis, there is lacunar collenchyma grouped into 10-15 rows on protruding parts (Figure 6). The collenchyma cells join the chlorenchyma cells along the stem. There are 19-41 oil granules and 13-17 rows of parenchyma cells in the outmost areas of the cortex. The vascular bundles embedded in the sclerenchyma are arranged in a ring (Figure 6). In the main region, parenchyma cells with a size of 41.22×44.67 µm and secretory ducts are located.

Most of the conductive bundles in the stem cortex, which are usually circular in shape, have oil ducts. Parenchyma cells expand from the cortex to the core. Sclerenchyma cells nearly penetrate the conductive bundles and form a ring. In the depression region there are large parenchyma cells with intercellular spaces and oil ducts. There are also samples without secretory ducts near the core (Figure 7).

Since the genus Conium has not been previously studied, we considered in more detail the species of the family Apiaceae.

Protrusions (veins) formed by swollen chyme cells, as mentioned in Ulusoy (2017) study, were found in a single locality (Karasai district), exclusively on stem cuttings. Chlorenechyma cells are located between the stem veins. In other specimens, these features were not observed. In general, the stem structure was quite similar.

According to Başer and Pehlivan, (2015), stem sections were round. Conductive bundles of the cortex layer had a single oil duct. The cortex layer contained parenchyma cells and the conductive bundles were along the stem within the sclerenchyma. Therefore, the sample was similar to the samples from our study.

In addition, according to Başer and Pehlivan, (2015), sclerenchyma cells were found in the cortex and phloem layers. This feature was not found in our localities. Finally, according to Başer and Pehlivan (2015), the taxa have a flock cap and the stem structure of our species, in contrast, is different.

According, the stem was round and striped. The epidermis consists of homogeneous, densely spaced horizontally oval, square or rectangular cells surrounded by a thick layer of cuticula. This cuticula is absent in our samples.

Also, in the sample of (Saltan, 2015), the upper and lower walls of the epidermis are thick and the lateral walls are thin. Under the epidermis, there is a well-developed collenchyma tissue from which the central vein emerges. This property is also observed in our samples. Under the epidermis, between the collenchyma tissue that makes up the outer part of the cortex, there is the chlorenchyma tissue (photosynthetic tissue) consisting of parenchyma cells. After the collenchyma layer, there is a secretory duct. Inside the cortex,

parenchyma tissue forms a ring. Below is a ring formed by sclerenchyma tissue. The collateral conductive bundles are partially separated by basal parenchyma and sclerenchyma. Near the core, the parenchyma tissue fragments and the center of the stem becomes hollow. These features were mostly consistent with our samples.

Results of the Statistical Analysis

Mean ± standard deviation, minimum and maximum values and 95% confidence interval were estimated using ANOVA and Turkey test. The analyses revealed significant differences between taxa. ANOVA revealed significant differences in 26 stem characters (Table 6). Turkey analysis yielded similar results. The following elements were not significantly different: G1, G10, G23, G28 and G30 (Fig 8-10).

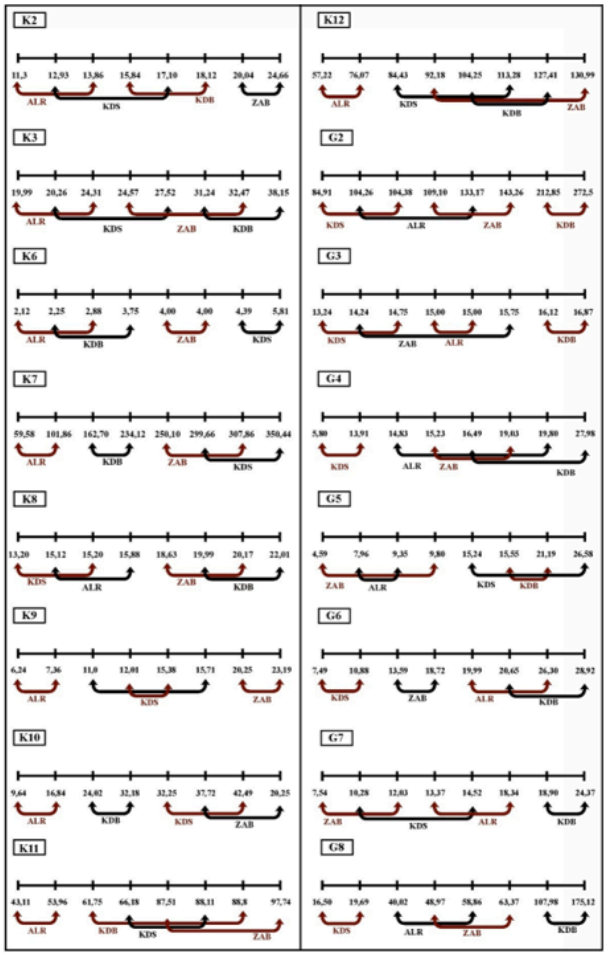

Fig. 8: Symbols of the root and stem grouped according to measurement statistics

Kaya & Başer (2002); Kaya (2003) (*Astrantia* L.), (Saltan, 2015) (Crenosciadium siifolium and Glaucosciadium cordifolium), Ulusoy (2017) (Caropodium Stapf & Wettst.) and Başer and Pehlivan (2015) (Grammosciadium DC.) observed similar stem anatomical features. A cavity in the nucleus of the genus Astrantia L. is also found in some parts of *C. maculatum.* The general characterization of the Apiaceae family (Metcalf & Chalk, 1965) is similar to our findings, including secretory tubes inserted into the parenchyma, the arrangement of conducting bundles in a ring on the stem and their separation from the main tissues (Fischer *et al.*, 2008; Tleuberlina *et al.*, 2023; Walker, 1959).

Significant differences were found between root and stem marks in samples collected from different regions. Therefore, it would be useful to conduct comparative studies with many samples from the same area to better understand the importance of anatomical features.

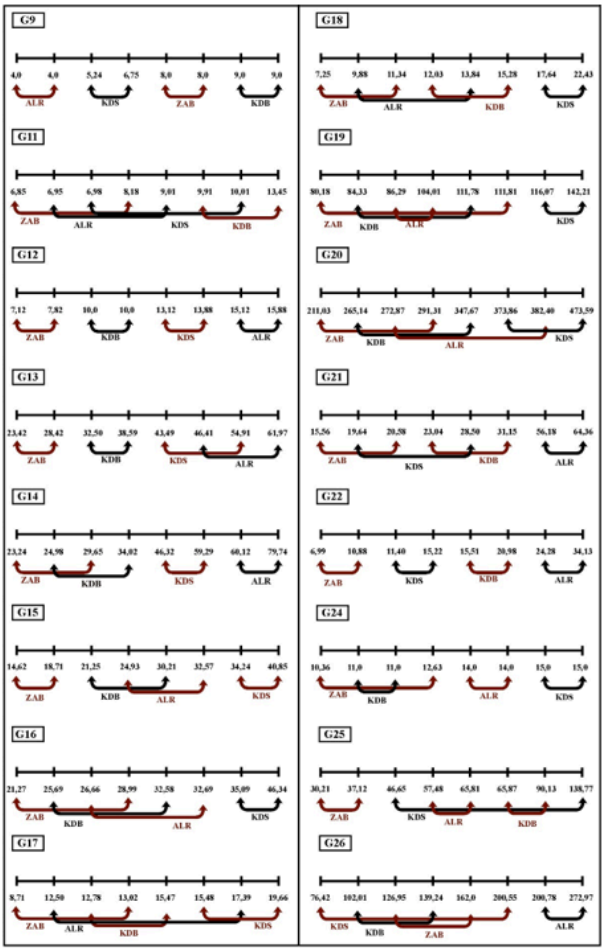

Fig. 9: Symbols of the root and stem grouped according to measurement statistics

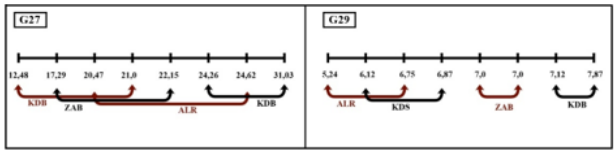

Fig. 10: Symbols of the root and stem grouped according to measurement statistics

Conim maculatum L. contains piperidine alkaloids (coniine, N-methyl-coniine, conhydrine, pseudoconhydrine, gamma-coniine), which are formed because of cyclization of an eight-carbon chain

originating from four acetate units. Gamma-Coniceine is a precursor of other hemlock alkaloids. All vegetative organs, flowers and fruits contain alkaloids. The concentration (both absolute and relative) of different alkaloids depends on the plant variety, environmental conditions and the plant age. Conmaculatin (2-Pentylpiperidine), a novel volatile alkaloid related to coniine, has been identified from *C. maculatum.*

Table 6: Stem anatomical features and results of the statistical analysis

Description		Almaty Nature Reserve 10.07.2021 (B4) N=10	Karasai District (Shamalgan)14.07.2021 (B3) N=10	Karasai District 13.05.20 (B1) N=10	Zailiyskiy Alatau 1.07.2021(B2) N=10 43°03′ , 77°15′
G1	Ort ± Std	3100,4 ±68,94	2941,4±48,27	2179,7±112,32	1963,4±120,53
	min-max	29513195	2862-3000	1996-2367	1805-2142
	95% CI	3051,083149,7	2906,8-2975,9	2099,3-2260,0	1877,17-2049,62
G2*	Ort ± Std	118,72±20,20^{A}	93,64±15,0^{A}	242,68±41,69^{B}	126,18±23,87^{A}
	min-max	90,61152,30	71,10114,90	183,30306,70	90,02159,4
	95% CI	104,26133,17	82,91104,38	212,85272,50	109,10143,26
G3*	Ort ± Std	15,0±0,0^{B}	14,0 ±1,05^{A}	16,5±0,5^{C}	15,0±1,05^{B}
	min-max	15,015,0	13,015,0	16,0-17,0	14,016,0
	95% CI	15,015,0	13,2414,75	16,1216,87	14,2415,75
G4*	Ort ± Std	17,32±3,47^{B}	9,86 ±5,67^{A}	21,93±7,6^{B}	17,13±2,65^{B}
	min-max	12,2821,54	5,0121,05	10,8733,38	12,0020,67
	95% CI	14,8319,8	5,813,91	16,4927,38	15,2319,03
G5*	Ort ± Std	8,66±0,97^{A}	20,91±7,92^{B}	18,37±3,93^{B}	7,20±3,64^{A}
	min-max	7,54-10,77	13,19-35,75	12,37-24,00	3,67-16,33
	95% CI	7,96 -9,35	15,24 -26,58	15,55 -21,19	4,59 -9,8
G6*	Ort ± Std	23,15±4,40^{C}	9,18±2,36^{A}	24,78±5,78^{C}	16,16±3,57^{B}
	min-max	15,3329,66	6,8512,36	17,2537,13	10,8723,25
	95% CI	19,9926,30	7,4910,88	20,6528,92	13,5918,72
G7*	Ort ± Std	15,86±3,46^{B}	12,40±2,96^{BA}	21,63±3,82^{C}	9,78±3,13^{A}
	min-max	10,3021,36	8,1616,32	16,5027,38	6,3815,94
	95% CI	13,3718,34	10,2814,52	18,9024,37	7,5412,03
G8*	Ort ± Std	49,84±12,60^{B}	18,10±2,23^{A}	141,55±46,92^{C}	56,17±10,06^{B}
	min-max	21,6766,68	15,0021,00	90,02223,10	40,0171,68
	95% CI	40,8258,86	16,5019,69	107,98175,12	48,9763,37
G9*	Ort ± Std	4,0±0,0^{A}	6,0±1,05^{B}	9,0±0,0^{D}	8,0±0,0^{C}
	min-max	4,04,0	5,07,0	9,09,0	8,08,0
	95% CI	4,04,0	5,246,75	9,09,0	8,08,0
G10	Ort ± Std	7,93±1,30^{AB}	9,35±2,13^{B}	8,38±1,93^{B}	6,28±1,32^{A}
	min-max	5,549,69	7,0314,46	5,4411,81	4,008,50
	95% CI	7,018,87	7,8310,87	6,999,76	5,337,23
G11*	Ort ± Std	7,98±1,44^{A}	8,49±2,11^{A}	11,68±2,47^{B}	7,51±0,9^{A}
	min-max	5,089,69	6,1011,78	7,3115,75	6,179,0
	95% CI	6,959,01	6,9810,01	9,9113,45	6,858,18
G12*	Ort ± Std	15,5±0,5^{D}	13,5±0,5^{C}	10,0±0,0^{B}	7,5±0,5^{A}
	min-max	15,016,0	13,014,0	10,010,0	7,08,0
	95% CI	15,1215,87	13,1213,87	10,010,0	7,127,87
G13*	Ort ± Std	54,19±10,87^{C}	49,2±7,98^{C}	35,55±4,25^{B}	25,92±3,49^{A}
	min-max	38,3174,78	32,5760,01	31,5044,01	19,7530,0
	95% CI	46,4161,97	43,4954,91	32,5038,59	23,4228,42
G14*	Ort ± Std	69,93±13,71^{C}	52,8±9,06^{B}	29,5±6,31^{A}	26,45±4,48^{A}
	min-max	48,9388,17	36,86-63,44	23,0-41,51	20,75-34,25
	95% CI	60,1279,74	46,32-59,29	24,98-34,02	23,24-29,65
G15*	Ort ± Std	28,75±5,34^{B}	37,54±4,62^{C}	25,73±6,25^{B}	16,66±2,86^{A}
	min-max	22,1539,70	29,1545,43	14,6735,34	14,023,3
	95% CI	24,9332,57	34,2440,85	21,2530,21	14,6118,71
G16*	Ort ± Std	29,68±4,21^{A}	40,72±7,85^{B}	29,13±4,8^{A}	25,13±5,4^{A}
	min-max	23,5436,93	28,2953,15	20,67-34,0	16,6733,34
	95% CI	26,6632,69	35,0946,34	25,6932,57	21,2728,99
G17*	Ort ± Std	14,95±3,41^{B}	17,57±1,93^{B}	14,13±1,88^{AB}	10,86±3,01^{A}
	min-max	11,0721,69	12,8622,67	12,018,0	6,8416,71
	95% CI	12,5017,39	15,4719,66	12,7815,47	8,7113,02

Table 6 Continued: Stem anatomical features and results of the statistical analysis

Description		Almaty Nature Reserve 10.07.2021 (B4) N=10	Karasai District (Shamalgan)14.07.2021 (B3) N=10	Karasai District 13.05.20 (B1) N=10	Zailiyskiy Alatau 1.07.2021(B2) N=10 43°03′ , 77°15′
G18*	Ort ± Std	11,86±2,76^{AB}	20,03±3,34^{C}	13,66±2,27^{B}	9,3±2,85^{A}
	min-max	7,39-15,69	15,43-26,57	9,34-17,33	5,33-13,28
	95% CI	9,88 -13,84	17,64 -22,43	12,03 -15,28	7,25 -11,34
G19*	Ort ± Std	95,15±12,37^{A}	129,14±18,26^{B}	98,06±19,18^{A}	95,99±22,10^{A}
	min-max	80,0120,0	105,6170,4	73,14140,60	60,01141,4
	95% CI	86,29104,01	116,07142,2	84,33111,78	80,18111,81
G20*	Ort ± Std	327,64±76,55^{A}	423,73±69,70^{B}	306,41±57,68^{A}	251,17±56,11^{A}
	min-max	230,0461,6	316,0522,10	228,8388,2	186,4347,2
	95% CI	272,87382,40	373,86473,59	265,14347,67	211,03291,3
G21*	Ort ± Std	60,57±6,14^{C}	24,07±6,19^{AB}	27,10±5,66^{B}	18,07±3,50^{A}
	min-max	51,5568,74	12,7532,57	16,5035,25	13,2023,70
	95% CI	56,1864,96	19,6428,50	23,0431,15	15,5620,58
G22*	Ort ± Std	29,21±6,88^{C}	13,31±2,66^{AB}	18,25±3,82^{B}	8,94±2,71^{A}
	min-max	21,4842,96	9,7518,0	13,5025,0	5,4013,5
	95% CI	24,2834,13	11,4015,22	15,5120,98	6,9910,88
G23	Ort ± Std	41,0±0,0	19,0±0,0	19,0±0,0	22,0±0,0
	min-max	41,041,0	19,019,0	19,019,0	22,0022,0
	95% CI	41,041,0	19,019,0	19,019,0	22,0022,0
G24*	Ort ± Std	14,0±0,0^{B}	15,0±0,0^{C}	11,0±0,0^{A}	11,50±1,58^{A}
	min-max	14,014,0	15,015,0	11,011,0	10,0013,0
	95% CI	14,014,0	15,015,0	11,011,0	10,3612,63
G25*	Ort ± Std	61,64±5,82^{AB}	92,71±64,38^{B}	78,0±16,95^{B}	33,67±4,83^{A}
	min-max	51,5573,03	29,62197,0	58,34110,0	25,038,34
	95% CI	57,4865,81	46,65138,77	65,8790,13	30,2137,12
G26*	Ort ± Std	236,88±50,45^{B}	138,49±86,75^{A}	120,63±26,01^{A}	144,48±24,49^{A}
	min-max	165,4309,3	37,03244,40	95,02-183,70	100,0178,0
	95% CI	200,78272,9	76,42200,55	102,01139,24	126,95162,0
G27*	Ort ± Std	22,55±2,90^{BC}	27,65±4,73^{C}	16,74±5,95^{A}	19,72±3,39^{AB}
	min-max	16,4027,34	18,033,0	9,023,33	15,7526,25
	95% CI	20,4724,62	24,2631,03	12,4821,0	17,2922,15
G28	Ort ± Std	24,87±5,02	23,85±3,6	18,75±8,47	19,95±4,75
	min-max	17,77-34,17	18,0-28,0	8,25-29,34	12,75-25,5
	95% CI	21,28 -28,47	21,26 -26,43	12,68 -24,81	16,54 -23,35
G29*	Ort ± Std	6,0±1,05^{A}	6,5±0,5^{AB}	7,5±0,5^{C}	7,0±0,0^{BC}
	min-max	5,07,0	6,07,0	7,08,0	7,07,0
	95% CI	5,246,75	6,126,87	7,127,87	7,07,0
G30	Ort ± Std	13,0±0,0	8,0±0,0	11,0±0,0	14,0±0,0
	min-max	13,013,0	8,08,0	11,011,0	14,0014,0
	95% CI	13,013,0	8,08,0	11,011,0	14,0014,0

Chemical analysis showed that all *C. maculatum* tissues are rich in alkaloids, with the highest alkaloid content of up to 1% (w/w) found in fruits. The amount and the relative shares of several different alkaloids depend on the plant variety, environmental conditions and the development stage. *C. maculatum* also contains flavonoids, coumarins, polyacetylenes, vitamins and essential and non-volatile oils. The oil of *C. maculatum* grown in Iran was characterized by an increased content of germacrene-D (46.1%), β-caryophyllene (15.3%) and cis-α-Farnesene (10.1%).

C. maculatum is a biennial herbaceous plant (under favorable conditions - perennial; stems are bare, 0.6 to 2 m high, erect and hollow, except for nodes, grooved, branched, with numerous purple spots. The leaves are petiolate, pinnate-complex.

An important criterion in the study of poisonous plants is the persistence of a species in a particular area. This criterion is influenced by many factors, including anthropogenic factors, soil composition and the life form of the plant itself. Species with a longer life cycle (trees, shrubs, semi-shrubs, herbaceous perennials) can persist in the same place for decades. As for species with a short life cycle (annuals and biennials), their presence in the flora is unstable, which makes it difficult to control their distribution and naturalization.

GC-MS Analysis

Extracts of B1, B2, B3 and B4 collected from four different locations in the Almaty region led to the identification of several compounds: These compounds were identified using Gas Chromatography-Mass

Spectrometry (GC-MS) All components identified by GC-MS were detected in C maculatum L The various components present in the herb are shown in Figure 1 GC-MS analysis revealed that each extract sample contains a unique phytochemical composition In general, samples were composed mainly of fatty acids, alkaloids and fatty aldehydes Available publications provide information on the presence of alkaloids, which are one of the chemopreventive phytochemicals associated with cancer treatment that contain agents to inhibit and stop oncogenesis In our study, each sample contained up to 50 compounds The results showed the presence of fatty acids such as 9,12,15-octadecatrienoic acid, (Z,Z,Z)-linolenic acid, tetratriacontane, palmitic acid and octadecanoic acid Meanwhile, the 2,3-dihydroxypropyl ester in the B1 extract was found with the highest content of 1535%, which was higher than the 1469%, 129% and 464% of the other components The following bioactive compounds (1-methyl-2-piperidinmethanol, carboxylic acid, monoamide, N-methyl- and allyl ether) were found in higher amounts and in equal proportions in the other three extracts (B2, B3 and B4) The retention time and concentration (%) of the active phytocompounds are shown in Table (7) and C maculatum L ion chromatograms, in Figure (11).

Table 7: Bioactive compounds of C. maculatum L. found in samples B1, B2, B3 and B4

No.	Compound				Concentration, %				Retention time, min			
	B1	B2	B3	B4	B1	B2	B3	B4	B1	B2	B3	B4
1	Ethene, tetrachloro- (CAS)	Ethene, tetrachloro- (CAS)	Ethene, tetrachloro- (CAS)	Ethene, tetrachloro- (CAS)	0.64	0.28	0.15	0.14	5.714	5.71	5.72	5.71
2	Tetrachloroethylene	Tetrachloroethylene	1,2-dibromo-tetrachloro-	Coniine	2.13	1.18	0.41	0.93	5.843	5.824	5.843	11.297
3	2 (3H) - furanone, dihydro-3-hydroxy-4,4-dimethyl-,	Coniine	Coniine	1-Methyl-2-piperidinemethanol	0.75	0.9	0.94	40.39	12.383	11.295	11.296	12.334
4	Pantolactone	1-Methyl-2-piperidinemethanol	1-Methyl-2-piperidinemethanol	2-Pyrolidinone, 1-methyl- (CAS)	2.62	40.19	41.31	1.25	12.468	12.316	12.326	12.541
5	2-Pyrolidinone, 1-methyl- (CAS)	2-Pyrolidinone, 1-methyl- (CAS)	2-Pyrolidinone, 1-methyl- (CAS)	Silane, dimethyl (3-methylbut-3-enyloxy) butoxy -	3.62	1.35	1.25	0.21	12.587	12.53	12.542	16.835
6	2,4 (1H,3)-pyrimidinedione, 5-methyl - (CAS) ss	6-Ethyl-3-trimethylsilyloxidecane	4-Dimethylsilyloxytridecane	Carbon dioxide, monoamide, N-metal -, allyl ether	0.39	0.21	0.18	30.21	13.739	16.821	16.833	17.821
7	2,3-dihydro-3,5-dihydroxy-6-methyl-4H-pyran-4-	Carbon dioxide, monoamide, N-metal -, allyl ether	Carbon dioxide, monoamide, N-metal -, allyl ether	4-Methylpiperidine propionates	0.33	29.66	30.57	0.26	15.839	17.811	17.817	18.05
8	2,3-Dihydro-benzofurane-phthalane	4-Methylpiperidine propionates	4-Methylpiperidine propionates	Benzaldehyde <2,4-dimethyl ->	1.55	0.35	0.27	0.25	18.125	18.04	18.046	18.146
9	Guaiacol <4-Vinyl->	Benzaldehyde, 2,4-dimethyl-	2,4-dimethylbenzaldehyde	1-methyl-2-ethoxycarbonyl-1-aza-cyclohexane	2.52	0.26	0.26	0.23	21.024	18.138	18.147	18.64
10	3,4-Dihydroxystyrene	Ethyl 1-methylpipecolinate	2-Pyrrolidinemethanamine, 1-ethyl- (CAS)	Butan-2-boron, 3-methyl-3- (2-oxopropylamino)-	0.61	0.27	0.27	0.65	24.434	18.622	18.631	18.994
11	Diphenylamine	Butan-2-boron, 3-methyl-3- (2-oxopropylamino)-	Carbon dioxide, monoamide, N-metal -, allyl ether	1-Di(tert-butyl)silyloxybutane	0.46	0.8	0.63	0.25	29.202	18.98	18.989	19.287
12	(-)-Loliolide	Piperazine, 2,5-dimethyl-3-(2-methylpropyl)-	1-Di(tert-butyl)silyloxybutane	1-Dodecanol (CAS)	0.59	0.35	0.25	0.13	32.65	19.113	19.286	25.32
13	9-Eicosene	1-Di(tert-butyl)silyloxybutane	2-Butyl(dimethyl)silyloxybutane	9-Eicosene	0.91	0.5	0.1	0.52	32.982	19.281	19.544	28.32
14	Neophytadiene	2-Butyl(dimethyl)silyloxybutane	1-Dodecanol	E-14- Hex	0.36	0.15	0.11	0.17	34.017	19.536	25.316	30.364
15	Phyton	1-Pentadecene	9-Eicosene	9-Eicosene	0.48	0.53	0.53	0.95	34.149	28.315	28.318	32.987
16	1,2- Benzene dicarboxylic acid , bis(2-metilpropil)	Hexadecane	Heptadecane	Octadecane	0.66	0.13	0.14	0.11	34.732	28.49	28.499	33.133
17	Tolycaine	E-14-Оналтылық	n-Tridecan-1-ol	Neophytadiene	0.34	0.16	0.15	0.14	35.556	30.365	30.361	34.02
18	Palmitic acid	9-Eicosene	1-Heptadian	3,7,11,15-Tetramethyl-2-hexadecen-1-ol	12.9	0.93	0.96	1.63	36.635	32.982	32.983	34.553
19	Eicosamethylcyclodecasyloxane	Neophytadiene	Octadecane	1,2- Benzenedicarbon acid, bis(2-methylpropyl) ester (CAS)	0.32	0.13	0.11	0.22	36.994	34.016	33.13	34.732
20	1-Nonadecene	3,7,11,15-Tetramethyl-2-hexadecen-1-ol	Neophytadiene	E-6-Octadec-1-olacetate	1.53	1.62	0.12	0.66	37.213	34.549	34.014	34.95
21	n-Nonadecanol-1	1,2- Benzenedicarboxylic acid, bis(2-methylpropyl) ester (CAS)	3,7,11,15-Tetramethyl-2-hexadecen-1-ol	Diethyl di (prop-2-enyl)-silane	0.71	0.19	1.66	0.65	39.005	34.729	34.552	36.311
22	Heneicosane	3,7,11,15-Tetramethyl-2-hexadecen-1-ol	1,2- Benzenedicarboxylic acid, bis(2-methylpropyl) ester (CAS)	n-hexadecanoic acid	0.58	0.56	0.21	2.28	39.293	34.947	34.73	36.59
23	2- Hexadec-1-ol, 3,7,11,15-tetramethyl -, [R-	Tetradecalactone <delta ->	E-6-Octadec-1-olacetate	1,2-benzenedicarbon acid, bis (2-methoxyethyl) ether (CAS)	1.25	0.64	0.62	0.31	39.607	36.308	34.95	36.7
24	9,12,15 - Octadecatrienoic acid, (Z,Z,Z) - SS linolenic acid	n-hexadecanoic acid	Tetradecalactone <delta ->	1-Nonadecene	15.35	1.82	0.62	0.77	40.178	36.582	36.308	37.212
25	Thiosulfate acid (H2S2O3), S-(2-aminoethyl) ether	1,2-Benzenedicarbon acid, bis (2-methoxyethyl) ether (CAS)	n-hexadecane acid	1-Heneicosanol	1.98	0.32	2.06	0.23	40.504	36.7	36.59	39
26	6,9,12-octadecatrienoic acid, phenyl methyl ether	1-Nonadecene	1,2-Benzenedicarboxylic acid, bis (2-methoxyethyl) ester (CAS)	Hexadecane (CAS)	1.19	0.75	0.27	0.3	40.674	37.208	36.703	39.291
27	1-Tetracosanol	Heptadecyl alcohol	1-Nonadecanol	9- Octadecene acid, methyl ether, (E)-	1.35	0.21	0.76	0.15	41.069	39	37.214	39.353
28	Tetracosane	Heneicosane	Eicosane (CAS)	Phytol	0.6	0.23	0.1	0.29	41.172	39.292	37.334	39.604
29	Octadecamethylcyclononasiloxane	Phytol	n-heptadecanol-1	9,12- Octadecadiene acid (Z,Z)-	0.32	0.26	0.23	0.97	42.628	39.606	38.999	39.996
30	Docosane	(Z,Z)-9,12- Octadecadiene acid	Heneicosane	Linoleic acid ethyl ether	0.48	0.67	0.16	2.29	42.967	39.995	39.291	40.125

DOI: 10.3844/ojbsci.2025.548.562

Table 7 Continued: Bioactive compounds of C. maculatum L. found in samples B1, B2, B3 and B4

No.	Compound				Concentration, %				Retention time, min			
	B1	B2	B3	B4	B1	B2	B3	B4	B1	B2	B3	B4
31	Bigenic alcohol	Z,Z-8,10-Hexadecadiene-1-ol	Phytol	Thiosulfate acid (H2S2O3), S-(2-aminoethyl) ether	0.38	2.05	0.27	0.28	44.608	40.121	39.608	40.479
32	Heptadecane	Thiosulfate acid (H2S2O3), S-(2-aminoethyl) ether	9,12- Octadecadiene acid (Z,Z)-	1-Tetracosanol (CAS)	0.32	0.43	0.8	0.36	44.693	40.479	39.998	41.066
33	Heptasiloxane, hexadecamethyl- (CAS)	Ethyl oleates	Linoleic acid ethyl ether	Heneicosane	0.38	0.19	1.92	0.18	45.095	40.606	40.127	41.163
34	1-Docosanol (CAS)	1-Tetracosanol (CAS)	1-Tetracosanol (CAS)	Tetracosane	0.36	0.36	0.35	0.16	46.245	41.063	41.064	42.963
35	Pentacosane	Docosane	Docosane	1-Heptacosanol	0.5	0.19	0.18	0.11	46.347	41.163	41.166	44.596
36	Hexadecenoic acid, 2-hydroxy-1-	Tetracosane	Tetracosane	SILICONE OIL	8.09	0.16	0.16	0.11	46.594	42.959	42.965	45.095
37	Benzyl diethyl (2,6-xylylcarbamoyl methyl)-	1-Heneicosanol	benzenedicarboxylic acid	Phenol, 2,2'-methylenebis[6-(1,1-dimethylethyl)-4-methyl-	0.93	0.19	0.13	0.82	47.147	44.595	44.601	45.248
38	1,2-Benzenedicarboxylic acid, bis(2-ethylhexyl) ester (CAS) ss Bis (2-ethylhexyl) phthalate	Phenol, 2,2'-methylenebis[6-(1,1-dimethylethyl)-4-methyl-	Eicosamethylcyclodecasyloxane	n-Tetracosanol-1	1.67	0.76	0.11	0.15	47.263	45.242	45.096	46.237
39	1H-purine-6-amine, [(2-fluorophenyl)methyl]-	1-Nonadecanol	Phenol, 2,2'-methylenebis[6-(1,1-dimethylethyl)-4-methyl-	Docosane	0.74	0.14	0.82	0.33	47.404	46.238	45.248	46.342
40	Triacontane	Pentacosane	1-Docosanol (CAS)	1,2-benzenedicarbon acid, bis(2-ethylhexyl) ether (CAS)	0.46	0.34	0.14	0.11	47.937	46.336	46.242	47.258
41	Nonacosane	Nonacosane	Pentacosane	Eicosamethylcyclodecasyloxane	0.95	0.13	0.32	0.13	48.912	47.927	46.343	47.403
42	2-methylhexacosane	Tetratriacontane	1,2-benzenedicarbon acid, bis(2-ethylhexyl) ether (CAS)	Tetratriacontane	3.65	1.39	0.1	1.33	49.463	49.463	47.256	49.469
43	Silicone oil	Tetracosanoic acid, methyl ether	1H-purine-6-amine, [(2-fluorophenyl)methyl]-	Tetracosanoic acid, methyl ether	0.93	0.35	0.11	0.35	49.574	49961	47.408	49.964
44	Octadecane acid, 2,3-dihydroxypropyl ether	Phytol acetate	Tetratriacontane	Isophytol acetate	4.64	0.14	1.29	0.14	49.838	50.588	49.466	50.594
45	1,3-benzenedicarbonal acid, bis(2-ethylhexyl)	Tetracontane	Tetracosanoic acid, methyl ether	Pentacosane	0.57	0.35	0.35	0.34	50.298	50.949	49.963	50.954
46	Pentatriacontane	Squalene	Phytol acetate	Squalene	0.56	0.4	0.14	0.39	50.956	51.5	50.594	51.503
47	Cyclodecasiloxane, eicosamethyl	Dotriacontane	Nonacosane	Tetracontane	0.42	6.39	0.34	6.68	51.601	52.39	50.952	52.398
48	Tetratriacontane	12-Tricosanone	Squalene	12-Tricosanone	14.69	0.15	0.39	0.14	52.403	55.199	51.501	55.199
49	Hexacosane (CAS)	Hexacosane (CAS)	Tetracontane	Triacontane	1.64	0.14	6.56	0.12	55.373	55.363	52.397	55.372
50	1-Eicosanol (CAS)	1-Eicosanol (CAS)	12-Tricosanone	1-Heptacosanol (CAS)	0.63	0.15	0.13	0.22	55.493	55.486	55.177	55.48

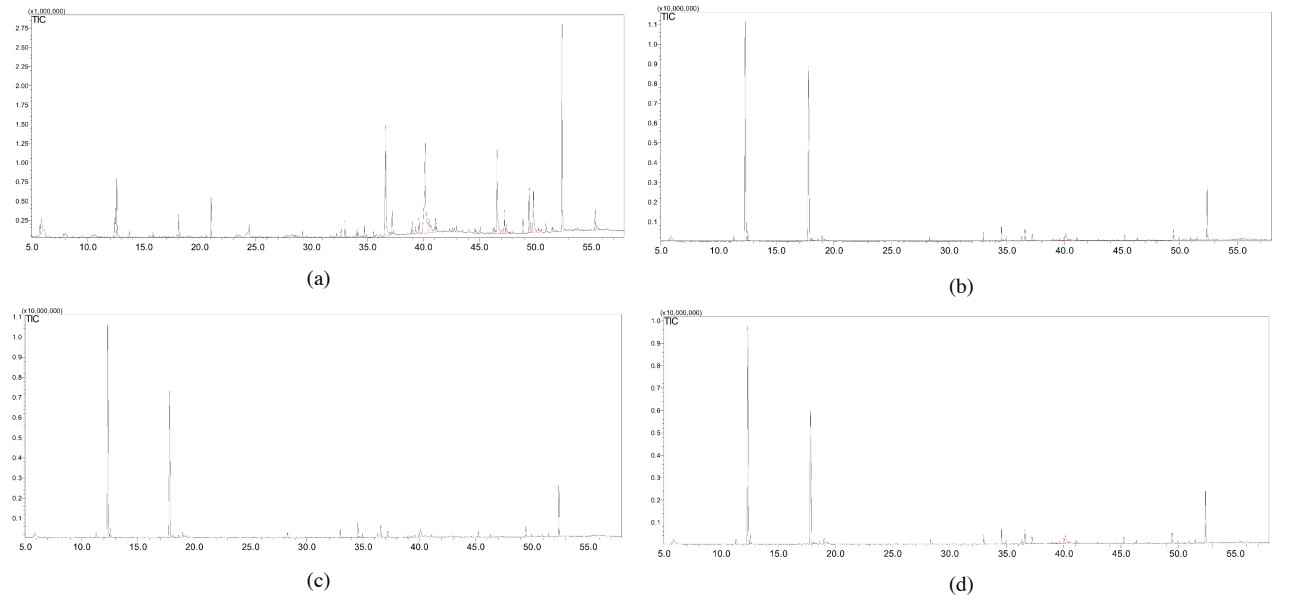

Fig. 11: Chromatograms of C. maculatum L. GC-MS from different populations: (a) B1; (b) B2; (c) B3; (d) B4

Among the bioactive components identified, palmitic acid and octadecanoic acid, 2,3-dihydroxypropyl ether were found in extract B1.

Palmitic acid has several biological properties, including antioxidant, hypocholes-terolemic, nematicidal and pesticidal. Octadecanoic acid, a 2,3-dihydroxypropyl ether, has antimicrobial and antitumor activity. Tetratriacontane with antioxidant and cytopro-tective activity was present in four *C. maculatum* L. plant samples.

The plant is used as an anesthetic in folk and official medicine in several countries in Europe (Austria, Germany, Greece, etc.) and America (Venezuela, Mexico and Chile).

In recent years, the interest in *C. maculatum* has been growing. Its potential uses include treatment of

abdominal pain, gastric ulcer, nervous excitement, nervousness and anxiety, as well as in the treatment of cancer.

In the study of *C. maculatum*, a macro- and microscopic method was used to obtain detailed information about the biological characteristics and structure of the plant, a histochemical method for studying the chemical composition and luminescent, chromatographic and spectrophotometric methods for determining phytochemical specificity.

For the first time, *C. maculatum* was studied in the mountainous areas of the Trans-Ili Alatau. The morphobiological features and medicinal properties of *C. maculatum* were studied:

1. Biological characteristics were described
2. Morpho-anatomical features were revealed
3. The chemical composition and phytochemical features were studied
4. The current state of the populations of *C. maculatum* in the foothills of the Trans-Ili Alatau was assessed

This article comprehensively analyzed the biological features of the medicinal plant *C. maculatum* L., its main distribution areas in the country and described the systematic classification, phytochemical features and chemical structure of the species. We demonstrated ecological and phytocenotic features of two populations of *C. maculatum* from the foothills of the Trans-Ili Alatau.

The paraffin method was used for anatomical studies of roots, stems and leaves of plants from different populations [45]. Anatomical studies were carried out in five stages, including dehydration, saturation, embedding, separation and staining.

Conclusion

The results obtained by examining cross-sections are crucial for determining the features of the anatomical structure. According to the available publications, the root, stem and leaf anatomy was very similar in all species of the family Apiaceae. However, idioblast cells, especially vessels, have been found to be diagnostic for the genus Caropodium. In addition, the formation of bast bundle fibers in the stems was a diagnostic character in the genera Caropodium and Grammosciadium. As a result of the literature search, no evidence of such characters was found in any other taxon of the family Apiaceae.

In our study, among taxa the characteristics of roots, stems and leaves did not differ. Thus, the obtained results are in line with the previous studies of the family Apiaceae. However, statistical analysis of quantitative characters revealed significant differences between taxa in most traits measured. Specifically, 35 of the 42 traits measured in this study showed significant differences.

According to our results, four extracts of *C. maculatum* have a remarkable antioxidant activity. *C. maculatum* TPC was used to determine the antioxidant activity of extracts. The data showed that the total amount of phenols in the B3 population was significantly higher (470.1 µg Gae/mL) than in the other samples and showed the highest antioxidant activity with 82.2% SA of the DPPH radical. GC-MS analysis revealed the presence of 50 phytochemical components with antimicrobial, antioxidant, antitumor, hypercholesterolemic, cytoprotective and other activities. From the point of view of the basic composition, B1 had completely different basic compounds compared to the others, while B2, B3 and B4 were identical.

Our studies have shown that in the future it is possible to introduce spotted hemlock into cultivation to meet the needs of homeopathy and scientific medicine in high-quality raw materials.

Author's Contributions

Aigerim Abdygalieva: Conceptualization, methodology.

Meruyert Kurmanbayeva: Writing-original draft preparation, supervision.

Dina Karabalayeva: Validation, data curation.

Zhumagali Ospanbayev: Investigation, visualization.

Moldir Zhumagul: Funding acquisition, writing-review and editing.

Almagul Aldibekova: Software, resources.

Adil Kusmangazinov: Formal analysis, project administration.

All authors have read and agreed to the published version of the manuscript.

Ethics

This article is original and contains unpublished material. The corresponding author confirms that all of the other authors have read and approved the manuscript and no ethical issues are involved.

Conflicts of Interest

The authors declare no conflicts of interest.

References

Akpulat, H. A., & Ataşlar, E. (2014). The Anatomical Structure of Endemic Peucedanum Graminifolium boiss.(Apiaceae/Umbelliferae. *Journal of Faculty of Pharmacy of Istanbul University*, *44*(2), 225-232.

Al-Barwani, F. M., & Eltayeb, E. A. (2004). Antifungal compounds from induced Conium maculatum L.plants. *Biochemical Systematics and Ecology*, *32*(12), 1097-1108. https://doi.org/10.1016/j.bse.2004.02.011

Alishah, H., Pourseyedi, S., Mahani, S. E., & Ebrahimipour, S. Y. (2016). Extract-Mediated Synthesis of Ag@Agcl Nanoparticles Using Conium Maculatum Seeds: Characterization, Antibacterial Activity and Cytotoxicity Effect Against Mcf-7 Cell Line. *RSC Advances*, *6*(77), 73197-73202. https://doi.org/10.1039/c6ra16127h

Al-Snafi, A. E. (2016). Pharmacology and Toxicology of Conium Maculatum-A Review. *The Pharmaceutical and Chemical Journal*, *3*(2), 136-142.

Bani, B., Karakaya, M. A., & Çeter, T. (2016). Fruit micromorphological characters of the genus Grammosciadium DC. (Apiaceae) in Turkey. *Phytotaxa*, *246*(3), 191-184. https://doi.org/10.11646/phytotaxa.246.3.2

Bani, B., Mavi, Ö., & Adıgüzel, Nezaket. (2011). Morphological and Anatomical Notes on a Local Endemic Species: Grammosciadium confertum Hub.-Mor. & Lamond Umbelliferae. *Biological Diversity and Conservation*, *4*(1), 1-6.

Bani, B., Ulusoy, F., Karakaya, M. A., & Koch, M. A. (2016). Taxonomic Implications from Morphological And Anatomical Studies in the Section Stenodiptera from the genus Grammosciadium (Apiaceae. *PhytoKeys*, *68*(9), 73-89. https://doi.org/10.3897/phytokeys.68.9089

Başer, B., & Pehlivan, S. (2015). Türkiye'nin Farklı Bölgelerindeki Prangos Lindl. (Apiaceae) Cinsine Ait Taksonların Polenlerinin Morfolojik Farklılıkları. *Bitlis Eren Üniversitesi Fen Bilimleri Dergisi*, *4*(2), 183-188. https://doi.org/10.17798/beufen.11965

Begum, B. S., & Mastan, M. (2015). Phytochemical Screening, Chromatographic analysis of Chloroform extract of Conium maculatum. *International Research Journal of Biological Sciences*, *4*(3), 27-29.

Chizzola, R., & Lohwasser, U. (2020). Diversity of Secondary Metabolites in Roots from Conium maculatum L. *Plants*, *9*(8), 939. https://doi.org/10.3390/plants9080939

Dayan, A. D. (2024). Death of Socrates: A Likely Case of Poison Hemlock (Conium maculatum) Poisoning. *Clinical Toxicology*, *62*(1), 56-60. https://doi.org/10.1080/15563650.2024.2309328

Durnova, N. A., Kuznetsova, I. A., & Potapova, A. S. (2019). Poisonic Vascular Plants of the City Saratov. *Bulletin of Botanic Garden of Saratov State University*, *17*(1), 39-54. https://doi.org/10.18500/1682-1637-2019-1-39-54

Filonova, M. V., & Medvedeva, Y. V. (2017). Cytogenetic Research of Conium Maculatum l. in Vitro and in Vivo. *Biotechnology: State and Prospects of Development*, *20*, 314.

Filonova, M. V., Shilova, I. V., Medvedeva, Y. V., & Churin, A. A. (2018). Chromatography-Mass Spectrometric Studies of Biologically Active Substances of *Conium Maculatum* l. Suspension Culture. *Book of Proceedings of the All-Russian Scientific Conference with International Participation and Schools of Young Scientists "Mechanisms of Resistance of Plants and Microorganisms to Unfavorable Environmental" (Parts I, II)*, 1411-1413. https://doi.org/10.31255/978-5-94797-319-8-1411-1413

Fischer, A. H., Jacobson, K. A., Rose, J., & Zeller, R. (2008). Cryosectioning Tissues. *Cold Spring Harbor Protocols*, *2008*(8). https://doi.org/10.1101/pdb.prot4991

Grudzinskaya, L. M., Gemejiyeva, N. G., & Karzhaubekova, Zh. Zh. (2020). The Kazakhstan Medicinal Flora Survey in a Leading Families Volume. *Bulletin of the Karaganda University "Biology Medicine Geography Series",100*(4), 39-51. https://doi.org/10.31489/2020bmg4/39-51

Hotti, H., Seppänen-Laakso, T., Arvas, M., Teeri, T. H., & Rischer, H. (2015). Polyketide Synthases from Poison Hemlock (Conium maculatum L.). *The FEBS Journal*, *282*(21), 4141-4156. https://doi.org/10.1111/febs.13410

Jha, S., Hajra, D., Chouni, A., & Paul, S. (2024). Novel Triterpenoid, Schidigeragenin b Resourced from the Mother Tincture of Conium Maculatum: A Promising Future Antidiabetic Drug. *Pharmacological Research - Natural Products*, *4*, 100077. https://doi.org/10.1016/j.prenap.2024.100077

Karakasi, M. V., Tologkos, S., Papadatou, V., Raikos, N., Lambropoulou, M., & Pavlidis, P. (2019). Conium Maculatum Intoxication: Literature Review and Case Report on Hemlock Poisoning. *Forensic Sci Rev*, *31*(1), 23-36.

Karakaya, M. A., Mavi İdman, Ö., & Bani, B. (2021). Detailed Fruit Anatomy of the Genus Grammosciadium DC. (Apiaceae). *Süleyman Demirel Üniversitesi Fen Bilimleri Enstitüsü Dergisi*, *25*(2), 395-400. https://doi.org/10.19113/sdufenbed.879586

Kaya, A. (2003). The genus Astrantia L. in Turkey: morphology and anatomy. *Acta Botanica Croatica*, *62*(2), 89-102.

Kaya, A., Başer, C., & Hüsnü, K. (2002). Olymposciadium Caespitosum (Umbelliferae): A Monotypic Endemic Species from Turkey. *Flora Mediterranea*, *12*, 377-387.

Khuda-Bukhsh, A., Mondal, J., & Panigrahi, A. (2014). Anticancer Potential of Conium Maculatum Extract Against Cancer Cells in Vitro: Drug-Dna Interaction and its Ability to Induce Apoptosis Through Ros Generation. *Pharmacognosy Magazine*, *10*(39), 524-533. https://doi.org/10.4103/0973-1296.139792

Kocabaş, O., Kayacan, E., Akyol, Y., Minareci, E., & Özdemir, C. (2015). Türkiye'de Yayılış Gösteren Hyparrhenia hirta (L.) Stapf (Poaceae) Türünün Anatomik Yapısının Belirlenmesi - The Anatomical Study on Hyparrhenia hirta (L.) Stapf (Poaceae) Species in Turkey. *Celal Bayar Üniversitesi Fen Bilimleri Dergisi*, *11*(2). https://doi.org/10.18466/cbujos.69198

Kumar, S., & Madaan, R. (2012). Screening of Alkaloidal Fraction of Conium Maculatum L. Aerial Parts for Analgesic and Antiinflammatory Activity. *Indian Journal of Pharmaceutical Sciences*, *74*(5), 457-460. https://doi.org/10.4103/0250-474X.108423

Kurmanbayeva, M., Rašeta, M., Sarsenbek, B., Kusmangazinov, A., Zhumagul, M., Karabalayeva, D., Altybayeva, N., Gafforov, Y., & Toishimanov, M. (2024). Comparison of fatty acids and amino acids profiles of the selected perennial and annual wheat varieties from Kazakhstan. *Natural Product Research*, 1-6. https://doi.org/10.1080/14786419.2024.2305654

Kusmangazinov, A., Kurmanbayeva, M. S., Zharkova, I., Karabalayeva, D., Kaparbay, R., & Kaiyrbekov, T. (2023). Comparison of Anatomical Characteristics and Phytochemical Components Between Two Species of Hedysarum (Fabaceae). *OnLine Journal of Biological Sciences*, *23*(3), 323-335. https://doi.org/10.3844/ojbsci.2023.323.335

Ligacheva, A. A., Sherstoboev, E. Yu., Danilets, M. G., Trofimova, E. S., Krivoshchekov, S. V., Gur'ev, A. M., Bulgakov, T. V., Kudashkina, N. V., Miroshnichenko, A. G., & Belousov, M. V. (2020). Study of Immunotropic Properties of Water-Soluble Polysaccharides Isolated from Conium Maculatum Grass. *Bulletin of Experimental Biology and Medicine*, *170*(2), 203-206. https://doi.org/10.1007/s10517-020-05033-y

Mavi Idman, D. Ö., Karakaya, M. A., Ulusoy, F., & Bani, B. (2019). Comparative vegetative anatomy of the genera Grammosciadium, Caropodium and Vinogradovia (Apiaceae) in Turkey. *Phytotaxa*, *427*(1), 9-21. https://doi.org/10.11646/phytotaxa.427.1.2

Meier, P., Hotti, H., & Rischer, H. (2015). Elicitation of Furanocoumarins in Poison Hemlock (conium maculatum l.) Cell Culture. *Plant Cell, Tissue and Organ Culture (PCTOC)*, *123*(3), 443-453. https://doi.org/10.1007/s11240-015-0847-7

Metcalfe, C. R., & Chalk, L. (1950). *Anatomy of the dicotyledons: leaves, stem, and wood in relation to taxonomy, with notes on economic uses*. *2*.

Miloud, M. M., & Senussi, N. A. (2023). Evaluation of Antibacterial Activity of Ethanolic Leaf Extracts of three Medicinal Plants Against Pathogenic Bacterial Species. *Scientific Journal of Applied*, 38-49.

Ouasti, M., Ouasti, I., Bussmann, R. W., & Elachouri, M. (2024). Conium maculatum L. Apiaceae. *Ethnobotany of Northern Africa and Levant*, 807-811. https://doi.org/10.1007/978-3-031-43105-0_82

Panter, K. E., Welch, K. D., & Gardner, D. R. (2017). Toxic Plants. *In Reproductive and Developmental Toxicology*, 903-923. https://doi.org/10.1016/b978-0-12-804239-7.00046-9

Pimenov, M. G. (2017). Updated Checklist of Chinese Umbelliferae: Nsynonymy, Typification, Distribution. *Turczaninowia*, *20*(2), 106-239. https://doi.org/10.14258/turczaninowia.20.2.9

Radulovic, N., & Djordjevic, N. (2011). Steroids from Poison Hemlock (Conium maculatum L.): A GC-MS analysis. *Journal of the Serbian Chemical Society*, *76*(11), 1471-1483. https://doi.org/10.2298/jsc110206128r

Salem, M. Z. M., Mohamed, A. A., Ali, H. M., & Al Farraj, D. A. (2021). Characterization of Phytoconstituents from Alcoholic Extracts of Four Woody Species and Their Potential Uses for Management of Six Fusarium oxysporum Isolates Identified from Some Plant Hosts. *Plants*, *10*(7), 1325. https://doi.org/10.3390/plants10071325

Saltan, N. (2015). *Crenosciadium Siifolium Ve Glaucosciadium Cordifolium (Apiaceae)'Un Farmasötik Botanik Yönünden Araştırmaları*.

Sayed-Ahmad, B., Talou, T., Saad, Z., Hijazi, A., & Merah, O. (2017). The Apiaceae: Ethnomedicinal family as source for industrial uses. *Industrial Crops and Products*, *109*, 661-671. https://doi.org/10.1016/j.indcrop.2017.09.027

Tamamschian, S. G., & Vinogradova, V. M. (1969). A Contribution to The Taxonomy of the Genus Grammosciadium Dc. *Umbelliferae. Bo-Tanicheskii Zhurnal (Leningrad*, *54*, 1197-1212.

Tleuberlina, O., Mamurova, A., Iskakova, Z., Aibuldinov, Y., Kolpek, A., Kopishev, Y., Satbaeva, G., Mukazhanova, Z., & Kurmanbayeva, M. (2023). Evaluation of the Capparis Herbacea Willd's Chemistry, Antioxidant and Cytotoxic Activity. *Anti-Inflammatory & Anti-Allergy Agents in Medicinal Chemistry*, *22*(4), 261-272. https://doi.org/10.2174/0118715230281697231115074426

Ulusoy, F., Karakaya, M. A., Mavi Idman, D. Ö., & Bani, B. (2017). A New Diagnostic Character in the Roots of the Genus Grammosciadium dc. (Apiaceae). *Phytotaxa*, *292*(2), 150-160. https://doi.org/10.11646/phytotaxa.292.2.2

Venkateswaran, S., Manivannan, H. P., Francis, A. P., Veeraraghavan, V. P., R, G., & Sankaran, K. (2023). Identification of Potential Phytochemical Inhibitors from Conium Maculatum Targeting the Epidermal Growth Factor Receptor in Metastatic Colorectal Cancer Via Molecular Docking Analysis. *Cureus*, *15*(10), 48000. https://doi.org/10.7759/cureus.48000

Vetter, J. (2004). Poison hemlock (Conium maculatum L.). *Food and Chemical Toxicology*, *42*(9), 1373-1382. https://doi.org/10.1016/j.fct.2004.04.009

Walker, W. S. (1959). A modification of the Carbowax Embedding Technique for Plant Tissue Tissue. *Proceedings of the Iowa Academy of Science*, *66*(1), 81-85.